Polycyclic Bis(*tert*-butylamido)cyclodiphosph(III)azane Complexes of Lithium and Magnesium: Their Syntheses, Molecular Structures, and Relationships to Isoelectronic Cyclodisilazane Derivatives

Ingo Schranz and Lothar Stahl*

Department of Chemistry, University of North Dakota, Grand Forks, North Dakota 58202-9024

Richard J. Staples

Department of Chemistry and Chemical Biology, Harvard University, Cambridge, Massachusetts 02138

Received September 19, 1997

Syntheses and single-crystal X-ray diffraction studies of the bis(*tert*-butylamino)cylodiphosphazane *cis*-[(^{t}BuNP)$_2$(^{t}BuNH)$_2$], **1a**, and its lithium and magnesium salts are described. The pristine molecule has crystallographic C_2 symmetry, both N−H groups being disposed in an endo fashion, and crystallizes in the monoclinic space group *P*2*/c* with unit cell dimensions (193 K) $a = 9.600(4)$ Å, $b = 5.904(4)$ Å, $c = 18.97(1)$ Å, $\beta = 101.09(3)°$, and $Z = 2$. Treatment of **1a** with ^{n}BuLi or (^{n}Bu)$_2$Mg in refluxing THF yielded the heterocubic *cis*-[(^{t}BuNP)$_2$(^{t}BuNLi·THF)$_2$], **2a**, and the seco-heterocubic {[(^{t}BuNP)$_2$(^{t}BuN)$_2$]Mg·(THF)$_2$}, **3a**, respectively**.** The crystal data (223 K) for the dilithio compound are monoclinic, space group $P2_1/c$, $a = 10.691(1)$ Å, $b = 15.827(2)$ Å, $c = 19.424(4)$ Å, $\beta = 105.617(7)°$, and $Z = 4$, and those for the magnesium derivative (213 K) are monoclinic, space group $P2_1/n$, $a = 10.6272(4)$ Å, $b = 17.6643(7)$ Å, $c = 16.3625(6)$ Å, $\beta = 90.46(3)°$, and $Z = 4$. The lithium and magnesium complexes are shown to be isostructural with isoelectronic cyclodisilazane species, and the development of a parallel coordination chemistry for both ligands is proposed.

We have recently begun investigating the transition-metal chemistry of bis(*tert*-butylamino)cyclodisilazane,[1] **1b**.[2] This heterocycle had been used previously[3] to stabilize main-group metals in unusual coordination environments, but its involved synthesis detracts somewhat from its ligating properties. While trying to improve the synthesis of **1b**, we realized that the cyclodiphosphazane[4] *cis*-[(^{t}BuNP)$_2$(^{t}BuNH)$_2$], **1a**, is, in a broader sense of the definition,[5] isoelectronic[6] with this cyclodisilazane. The synthesis of **1a** is straightforward,[7] however, and it seemed likely that silicon and phosphorus with covalent radii of 1.11 and 1.06 Å,[8] respectively, would form isoelectronic cages of almost identical dimensions. Herein we report our results on the syntheses and single-crystal X-ray diffraction studies of bis(*tert*-butylamino)cyclodiphosph(III)azane and two of its derivatives (see Chart 1), and we compare their structural parameters to those of isoelectronic bis(*tert*-butylamido)cyclodisilazane systems.

(1) The systematic name for this molecule is *cis*-2,4-di(*tert*-butylamino)-1,3-di(*tert*-butyl)-2,4-dimethylcylodisilazane.
(2) Grocholl, L.; Huch, V.; Stahl, L.; Staples, R.; Steinhart, P.; Johnson, A. *Inorg. Chem.* **1997**, *36*, 4451.
(3) (a) Veith, M.; Goffing, F.; Becker, S.; Huch, V. *J. Organomet. Chem.* **1991**, *406*, 105. (b) Veith, M.; Goffing, F.; Huch, V. *Chem. Ber.* **1988**, *121*, 943. (c) Veith, M.; Becker, S.; Huch, V. *Angew. Chem., Int. Ed. Engl.* **1989**, *28*, 1237. (d) Veith, M.; Goffing, F.; Huch, V. *Z. Naturforsch.* **1988**, *43b*, 846.
(4) The systematic name for this molecule is *cis*-2,4-di(*tert*-butylamino)-1,3-di(*tert*-butyl)-1,3,2,4-cylodiphosph(III)azane.
(5) In the strict sense of the definition, isoelectronic molecules must have the same number of electrons and the same number of heavy atoms (ref 6). The silicon derivatives, having two additional methyl substituents, are thus not strictly isoelectronic with the cyclodiphosphazanes, but their central cage is.
(6) Langmuir, I. *J. Am. Chem. Soc.* **1919**, *41*, 868.
(7) (a) Holmes, R. R.; Forstner, J. A. *Inorg. Chem.* **1963**, *2*, 380. (b) Hill, T. G.; Haltiwanger, R. C.; Thompson, M. L.; Katz, S. A.; Norman, A. D. *Inorg. Chem.* **1994**, *33*, 1770.
(8) Sanderson, R. T. *Inorganic Chemistry*; Reinhold: New York, 1967.

Experimental Section

General Considerations. All operations were performed under an atmosphere of argon or prepurified nitrogen on conventional Schlenk lines or in a glovebox. The hydrocarbon or ethereal solvents were predried over molecular sieves or CaH_2 and distilled under a nitrogen atmosphere from sodium or potassium benzophenone ketyl immediately before use. Phosphorus trichloride, *tert*-butylamine, *n*-butyllithium, and dibutylmagnesium were obtained from Aldrich and used as received.

Mass spectra were recorded on a VG Micromass 7070E-HF double-focusing spectrometer in the FAB mode, using an MNBA matrix, or in the electron ionization mode, using an accelerating potential of 70 eV. Except for the molecular ions, fragment peaks are quoted only if their relative intensities exceeded 10%. NMR spectra were recorded on a Varian VXR-300 spectrometer. ^{1}H NMR and ^{13}C NMR spectra are referenced relative to C_6H_5D (7.15 ppm) and C_6H_6 (128.0 ppm), respectively. Phosphorus signals are referenced relative to external $P(OEt)_3$ at +137.0 ppm, with shifts to higher frequency (lower field) given a more positive value. Melting points were recorded on a Mel-Temp melting point apparatus; they are uncorrected. Elemental analyses were performed by Desert Analytics Laboratory, Tucson, AZ.

Syntheses. *cis*-[(^{t}BuNP)$_2$(^{t}BuNH)$_2$], 1a. This is a modified procedure of the one originally reported by Holmes and Forstner.[7a] In a 2000-mL three-neck flask equipped with an inert gas inlet, a magnetic stirring bar, and a dropping funnel, 105 mL (1.00 mol) of *tert*-butylamine was dissolved in 500 mL of toluene. Phosphorus trichloride (16.4 mL, 0.188 mol), dissolved in 100 mL of toluene, was then added dropwise to the cooled (0 °C) *tert*-butylamine solution. A voluminous white precipitate of *tert*-butylammonium chloride appeared immediately. After the addition was complete the reaction mixture was refluxed for

S0020-1669(97)01201-9 CCC: $15.00
Published on Web 03/10/1998

Chart 1

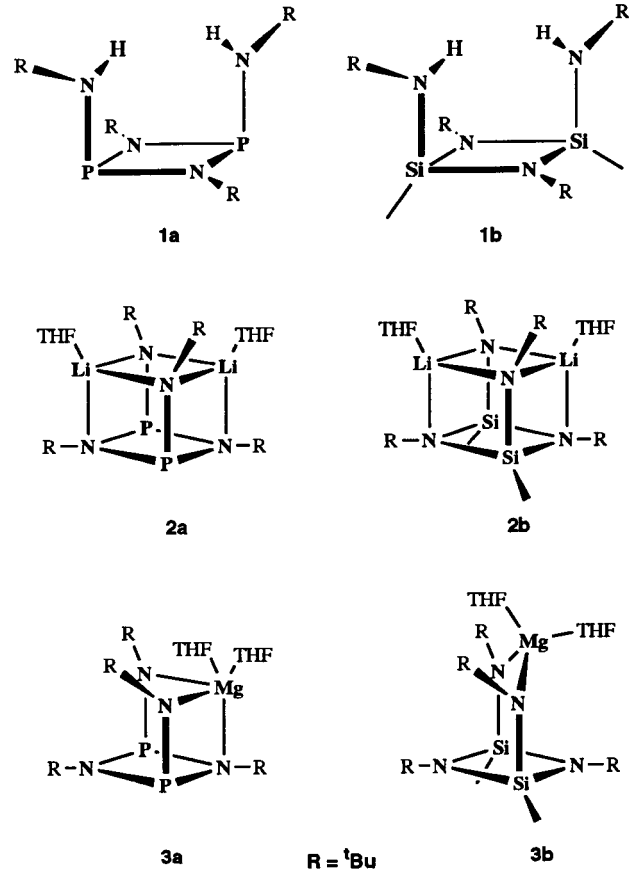

4 h, allowed to cool, and then filtered through a large (800-mL), coarse frit. The solid was washed with three 100-mL portions of toluene, and the combined filtrates were concentrated to about 90 mL. The flask was stored at −17 °C for 24 h, producing 27.5 g (0.0790 mol) of colorless, needle-shaped crystals of *cis*-[(ᵗBuNP)$_2$(ᵗBuNH)$_2$]. Yield: 84.0%.

Mp: 138 °C. ^{1}H NMR (300 MHz, benzene-d_6, 21 °C): δ 2.57 (d, 2H, J = 4 Hz), 1.44 (s, 18H, NᵗBu), 1.23 (s, 18H, NᵗBu). ^{13}C{^{1}H} NMR (75 MHz, benzene-d_6, 21 °C): δ 52.5 (t, J_{PC} = 23 Hz), 51.5 (d, J_{PC} = 19 Hz), 33.3 (d, J_{PC} = 10 Hz), 31.9 (t, J_{PC} = 7 Hz). ^{31}P{^{1}H} NMR (121 MHz, benzene-d_6, 21 °C): 88.5 (s). MS (EI, 70 eV): *m*/*z* (%) 57.1 (26.7), 58.1 (10.9), 103.1 (12.9), 108.0 (25.0), 123.1 (25.9), 164.1 (17.2), 220.1 (13.8), 276.1 (100.0), 277.1 (15.3), 348.1 (24.7 = M^+). Anal. Calcd for $C_{16}H_{38}N_4P_2$: C, 55.15; H, 10.99; N, 16.08. Found: C, 55.27; H, 11.02; N, 16.24.

***cis*-[(ᵗBuNP)$_2$(ᵗBuNLi·THF)$_2$], 2a.** Exactly 7.65 g (0.0220 mol) of *cis*-[(ᵗBuNP)$_2$(ᵗBuNH)$_2$], **1a**, was dissolved in 100 mL of THF in a 500-mL three-neck flask equipped with a magnetic stirring bar, two gas inlets, and a dropping funnel. Via cannula, 18.0 mL (0.0450 mol) of 2.5 M *n*-butyllithium solution was transferred to the dropping funnel and added dropwise to the cooled (0 °C) reaction vessel. After the reaction mixture had reached room temperature, it was refluxed for 3 h, allowed to cool, and reduced to 40 mL in vacuo. It was then stored at −17 °C for 2 days. This yielded 5.94 g (0.0118 mol) of very large, colorless rhombic crystals. Concentration of the supernatant to 15 mL, followed by storage at −17 °C for 4 days gave an additional crop, 2.63 g (0.00467 mol) of crystals. Overall yield: 74.8%.

Mp: 238 °C. ^{1}H NMR (300 MHz, benzene-d_6, 21 °C): δ 3.66 (t, 8H, OCH_2), 1.55 (s, 18H; NᵗBu), 1.49 (s, 18H, NᵗBu), 1.32 (q, 8H, CH_2). ^{13}C{^{1}H} NMR (75 MHz, benzene-d_6, 21 °C): δ 68.8 (s), 53.5 (t, J_{PC} = 15 Hz), 52.5 (d, J_{PC} = 26 Hz), 36.6 (d, J_{PC} = 12 Hz), 30.7 (t, J_{PC} = 7 Hz), 25.4 (s). ^{31}P{^{1}H} NMR (121 MHz, benzene-d_6, 21 °C): 159.6 (s). Anal. Calcd for $C_{24}H_{52}N_4Li_2O_2P_2$: C, 57.13; H, 10.39; N, 11.11. Found: C, 56.90; H, 10.26; N, 11.06.

{[(ᵗBuNP)$_2$(ᵗBuN)$_2$]Mg·(THF)$_2$}, 3a. A 100-mL three-neck flask equipped with gas inlet and dropping funnel was charged with 0.685 g (0.00135 mol) of *cis*-[(ᵗBuNP)$_2$(ᵗBuNH)$_2$], 30 mL of THF, and a magnetic stirring bar. Exactly 1.40 mL of 1.0 M dibutylmagnesium were transferred to the dropping funnel with a syringe and diluted to about 20 mL with hexanes. The flask was cooled to 0 °C, and the dibutylmagnesium reagent was added dropwise (1 drop/10 s) to the phosphazane solution. After the reaction mixture had warmed to room temperature, it was heated to reflux in an oil bath for 24 h. The solution volume was reduced to 10 mL in vacuo, and the flask was stored at −17 °C for 7 days. This afforded 0.440 g (0.855 mol, 63.0%) of colorless bar-shaped crystals of **3a**. These crystals become opaque under a vacuum, presumably due to the loss of THF.

Mp: 146−148 °C (dec). ^{1}H NMR (300 MHz, benzene-d_6, 21 °C): δ 3.71 (t, 8H), 1.59 (s, 18H, NᵗBu), 1.45 (s, 18H, NᵗBu), 1.32 (s, 8H). ^{13}C NMR (75 MHz, benzene-d_6, 21 °C): δ 69.1 (s), 52.8 (t, J_{PC} = 23 Hz), 52.5 (d, J_{PC} = 37 Hz), 36.6 (d, J_{PC} = 13 Hz), 31.6 (t, J_{PC} = 8 Hz), 25.2 (s). ^{31}P NMR (121 MHz, benzene-d_6, 21 °C): 119.46 (s). MS (FAB, MNBA): *m*/*z* (%) 56.9 (87), 57.9 (38), 62.8 (40), 76.9 (19), 78.9 (13), 88.9 (19), 89.9 (16), 90.9 (13), 102.0 (27), 103.1 (22), 106.9 (18), 107.9 (29), 118.9 (13), 119.9 (15), 123.0 (12), 124.0 (36), 136.1 (65), 137.1 (43), 138.2 (23), 154.1 (76), 155.1 (19), 159.1 (16), 164.1 (15), 174.1 (20), 180.1 (23), 204.2 (10), 220.2 (16), 236.2 (30), 276.3 (100), 277.3 (19), 292.2 (18), 307.2 (12), 348.3 (27), 349.3 (97), 350.3 (18), 364.3 (13), 365.3 (47), 379.3 (13), 516.4 (0.9 = M^+ + 1). Anal. Calcd for $C_{24}H_{52}N_4MgO_2P_2$: C, 55.98; H, 10.10; N, 10.88. Found: C, 56.14; H, 10.40; N, 10.92.

Single-Crystal X-ray Diffraction Studies. *cis*-[(ᵗBuNP)$_2$(ᵗBuNH)$_2$], 1a. A colorless, needle-shaped crystal of approximate dimensions 0.1 × 0.1 × 0.4 mm was attached to a glass capillary with silicone grease. Reflection intensities were collected with a Siemens SMART CCD (charge-coupled device) diffractometer equipped with an LT-2 low-temperature apparatus operating at 193 K. Data were measured using ω scans of 0.3° per frame for 30 s until a complete hemisphere had been collected. A total of 6200 reflections in 1271 frames were collected with a final resolution of 0.75 Å. The ranges of indices were $-12 \le h \le 11$, $-7 \le k \le 7$, $-25 \le l \le 16$, corresponding to a 2Θ range of 4.3−56.4°. These data were merged (R_{int} = 0.0547) to provide 2537 unique, observed ($I > 2\sigma(I)$) reflections. The first 50 frames were re-collected at the end of data collection to monitor for decay; none was observed. Cell parameters were retrieved using SMART[9] software and refined with SAINT on all observed reflections. Data reduction was performed with the SAINT software,[10] which corrects for Lp and decay. An empirical absorption correction based on the transmission factor range of 0.919−0.979 was applied using XEMP supplied in the SHEXTL-PC software. The structure was solved by direct methods in the space group *P*2*/c* (No. 13)—the acentric space group *Pc* was ruled out based on intensity statistics—with the SHELXS-90[11] program and refined by full-matrix least-squares methods on F^2 with SHELXL-93,[12] incorporated in SHELXTL-PC V 5.03.[13] All non-hydrogen atom positions were located in difference Fourier maps and refined anisotropically. Hydrogen atoms were placed in their geometrically generated positions and refined using a riding model.

***cis*-[(ᵗBuNP)$_2$(ᵗBuNLi·THF)$_2$], 2a.** Hardware configuration, data collection parameters, refinement procedure, and software used were identical to those used for **1a**. A total of 14 041 reflection intensities in 1271 frames were collected at 233 K with a final resolution of 0.75 Å. The index ranges were $-14 \le h \le 10$, $-20 \le k \le 19$, and $-18 \le l \le 25$, corresponding to a 2Θ range of 3.4−50.0°. These data were merged (R_{int} = 0.0492) to provide 5531 unique, observed ($I > 2\sigma(I)$) reflections. The first 50 frames were re-collected at the end of data collection to monitor for decay; none was observed. An empirical

(9) *SMART V 4.043 Software for the CCD Detector System*; Siemens Analytical Instruments Division: Madison, WI, 1995.
(10) *SAINT V 4.035 Software for the CCD Detector System*; Siemens Analytical Instruments Division: Madison, WI, 1995.
(11) Sheldrick, G. M. *SHELXS-90, Program for the Solution of Crystal Structures*; University of Göttingen: Göttingen, Germany, 1986.
(12) Sheldrick, G. M. *SHELXL-93, Program for the Refinement of Crystal Structures*; University of Göttingen: Göttingen, Germany, 1993.
(13) *SHELXTL 5.03 (PC-Version), Program Library for Structure Solution and Molecular Graphics*; Siemens Analytical Instruments Division: Madison, WI, 1995.

Scheme 1

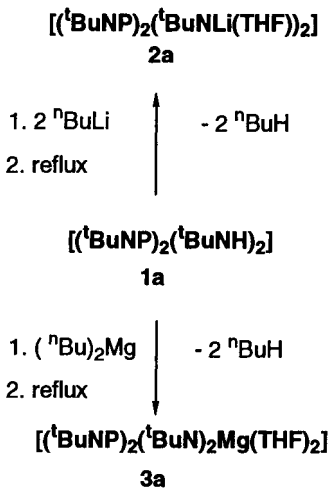

absorption correction based on a transmission factor range of 0.938−0.968 was applied. The structure was solved by direct methods in the unambiguous space group $P2_1/c$ (No. 14). A final difference Fourier map revealed no peaks (holes) greater than 0.293 (−0.431) e A^{-3}.

{[(tBuNP)$_2$(tBuN)$_2$]Mg·(THF)$_2$}, 3a. A colorless crystal of approximate dimensions 0.05 × 0.15 × 0.25 mm was attached to the inside of a thin-walled, nitrogen-filled glass capillary and transferred to the diffractometer. Hardware configuration, data collection parameters, and software programs were identical to those used for **1a** and **2a**. Compound **3a** crystallizes in the unambiguous space group $P2_1/n$ (No. 14). A total of 12 015 reflections were collected at 213 K, with a final resolution of 0.75 Å. The index ranges were $-12 \le h \le 12$, $-20 \le k \le 20$, and $-12 \le l \le 19$, corresponding to a 2Θ range of 3.4−50.0°. These data were merged ($R_{int} = 0.0417$) to provide 4988 unique, observed ($I > 2\sigma(I)$) reflections. An empirical absorption correction based on a transmission factor range of 0.695−0.970 was applied. A final difference Fourier map revealed no peaks (holes) greater than 0.801 (−0.320) e $Å^{-3}$.

Results

Synthetic routes to the cyclodiphosph(III)azane **1a** have appeared previously, but the reported procedures are either too cumbersome[7a] or too terse.[7b] Addition of phosphorus trichloride to *tert*-butylamine in a 1 to 5 molar ratio, eq 1, followed by a

$$2PCl_3 + 10H_2N^tBu \xrightarrow[\text{reflux, 3h}]{\text{toluene}} \underset{\mathbf{1a}}{[(^tBuNP)_2(^tBuNH)_2]} + 6(H_3N^tBu)Cl \quad (1)$$

3-h reflux and the removal of the ammonium chloride by filtration, afforded **1a** in analytically pure form. Although in principle any hydrocarbon or ethereal solvent may be used for this synthesis, toluene gave the best yields. The air-stable cyclodiphosph(III)azane was isolated in the form of square plates (hexane) or needles (THF, toluene) in yields exceeding 80%.

The cyclodiphosphazane can be metalated with strong bases such as *n*-butyllithium and dibutylmagnesium, as shown in Scheme 1. The lithiation was complete after 3 h of reflux and the dilithio salt was isolated as a bis(THF) adduct in typical yields of about 75%. Metalation of **1a** with dibutylmagnesium was slow, however, and only prolonged reflux in THF of up to 24 h allowed the isolation of spectroscopically and analytically pure **3a**, which crystallizes as a bis(THF) adduct. These highly crystalline, air-sensitive salts are convenient starting materials for a wide variety of main-group and transition-metal complexes of the cyclodiphosphazane.

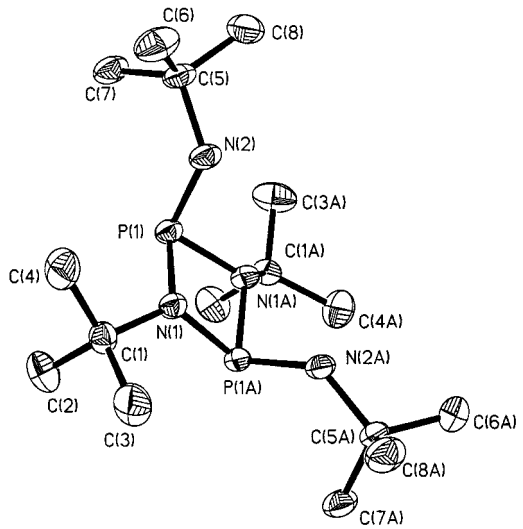

Figure 1. Perspective view of **1a**. The 50% probability thermal ellipsoids are shown.

Table 1. Crystallographic Data for **1a**−**3a**

	1a	2a	3a
empirical formula	$C_{16}H_{38}N_4P_2$	$C_{24}H_{52}N_4Li_2O_2P_2$	$C_{24}H_{52}N_4MgO_2P_2$
fw	348.44	504.52	514.95
space group	$P2_1/c$ (No. 13)	$P2_1/c$ (No. 14)	$P2_1/n$ (No. 14)
lattice constants			
a, Å	9.600(4)	10.691(1)	10.6272(4)
b, Å	5.904(4)	15.827(2)	17.6643(7)
c, Å	18.97(1)	19.424(4)	16.3625(6)
β, deg	101.09(3)	105.617(7)	90.47(3)
V, $Å^3$	1055(1)	3165.2(9)	3071.5(2)
Z	2	4	4
ρ (calc), g cm^{-3}	1.097	1.059	1.114
λ, Å	0.710 73	0.710 73	0.710 73
temp, K	193(2)	233(2)	213(2)
μ, cm^{-1}	2.10	1.61	1.87
R^a	0.0657	0.0663	0.0797
$R_w{}^b$	0.1452	0.1658	0.2212

$^a R = \sum|F_o - F_c|/\sum|F_o|$. $^b R_w = \{[\sum w(F_o - F_c)^2]/[\sum w(F_o)^2]\}^{1/2}$; $w = 1/[\sigma^2(F_o)^2+(0.1101P)^2 + 0.3597P]$, where $P = (F_o^2 + 2F_c^2)/3$.

The NMR spectroscopic data (^1H, ^{13}C, ^{31}P) for **1a** are summarized in the Experimental Section. With the exception of the previously unpublished ^{13}C NMR data, they are in agreement with those reported elsewhere.[7b] The ^1H NMR spectrum of **1a** displays one doublet and two singlets at δ 2.56, 1.45, and 1.22, corresponding to the NH, the *tert*-butylamino, and *tert*-butylimino groups, respectively. The ^1H NMR spectra of **2a** (**3a**) are composed of two sharp lines of equal intensities at δ 1.55 (1.60) and 1.49 (1.47). While the spectrum of the lithium derivative can be readily interpreted in terms of the C_{2v} symmetry of the molecule, that of **3a** can be reconciled only with a fluxional movement of the magnesium atom between N(1) and N(2) in solution. Two sets of multiplets for coordinated THF were also observed in both spectra; those of **3a** were broadened by the dynamic processes. None of the proton signals of **2a** and **3a** display coupling to the phosphorus nuclei. The single peak observed in the $^{31}P\{^1H\}$ NMR spectra of these compounds appears in a range, δ 119.5−159.6, that is typical for P(III) derivatives.

An ORTEP diagram of the cyclodiphosph(III)azane **1a** is shown in Figure 1; the crystal parameters and the bond lengths and angles are collected in Tables 1 and 2, respectively. The isolated molecules are stacked along the *b*-axis of the monoclinic unit cell and have crystallographically imposed C_2 symmetry, but they are almost C_{2v}-symmetric. Both NH groups are in an

Table 2. Selected Bond Lengths and Angles for **1a**−**3a**

1a

Bond Lengths (Å)		Bond Angles (deg)	
P(1)−N(2)	1.664(2)	N(2)−P(1)−N(1)	104.69(11)
P(1)−N(1)	1.721(2)	N(2)−P(1)−N(1A)	105.03(11)
P(1)−N(1A)	1.730(2)	N(1)−P(1)−N(1A)	80.88(11)
P(1)−P(1A)	2.600(2)	N(2)−P(1)−P(1A)	117.67(8)
N(1)−C(1)	1.485(3)	C(1)−N(1)−P(1)	124.8(2)
N(2)−C(5)	1.470(3)	C(1)−N(1)−P(1A)	125.1(2)
		P(1)−N(1)−P(1A)	97.83(11)
		C(5)−N(2)−P(1)	130.2(2)

2a

Bond Lengths (Å)			
P(1)−N(4)	1.654(2)	P(1)−N(2)	1.772(2)
P(1)−N(1)	1.785(2)	P(2)−N(3)	1.647(2)
P(2)−N(2)	1.772(2)	P(2)−N(1)	1.783(2)
Li(1)−O(1)	1.959(5)	Li(1)−N(4)	2.090(5)
Li(1)−N(3)	2.094(5)	Li(1)−N(1)	2.104(5)
Li(2)−O(2)	1.955(5)	Li(2)−N(4)	2.077(5)
Li(2)−N(3)	2.081(5)	Li(2)−N(2)	2.121(5)

Bond Angles (deg)			
N(4)−P(1)−N(2)	98.67(11)	N(4)−P(1)−N(1)	100.33(11)
N(2)−P(1)−N(1)	82.82(10)	N(3)−P(2)−N(2)	98.65(10)
N(3)−P(2)−N(1)	100.23(11)	N(2)−P(2)−N(1)	82.86(10)
N(4)−Li(1)−N(3)	99.6(2)	N(4)−Li(1)−N(1)	78.1(2)
N(3)−Li(1)−N(1)	77.7(2)	N(4)−Li(2)−N(3)	100.4(2)
N(4)−Li(2)−N(2)	76.5(2)	N(3)−Li(2)−N(2)	76.2(2)
P(2)−N(1)−P(1)	96.50(10)	P(1)−N(1)−Li(1)	88.6(2)
P(2)−N(1)−Li(1)	88.8(2)	P(1)−N(2)−Li(2)	89.8(2)
P(2)−N(2)−P(1)	97.38(10)	P(2)−N(2)−Li(2)	89.92(14)
P(2)−N(3)−Li(2)	94.9(2)	Li(2)−N(3)−Li(1)	75.5(2)
P(2)−N(3)−Li(1)	93.0(2)	P(1)−N(4)−Li(2)	94.7(2)
P(1)−N(4)−Li(1)	92.8(2)	Li(2)−N(4)−Li(1)	75.7(2)

3a

Bond Lengths (Å)			
Mg−N(3)	2.061(4)	Mg−N(4)	2.059(4)
Mg−O(1)	2.095(4)	Mg−O(2)	2.070(4)
Mg−N(1)	2.330(4)	Mg−P(1)	2.813(2)
Mg−P(2)	2.817(2)	P(1)−N(3)	1.654(4)
P(1)−N(2)	1.748(4)	P(1)−N(1)	1.782(4)
P(1)−P(2)	2.694(2)	P(2)−N(4)	1.658(4)
P(2)−N(2)	1.760(2)	P(2)−N(1)	1.778(4)

Bond Angles (deg)			
N(3)−Mg−N(4)	124.6(2)	N(4)−Mg−O(2)	113.1(2)
N(3)−Mg−O(2)	115.7(2)	N(4)−Mg−O(1)	101.8(2)
N(3)−Mg−O(1)	101.2(2)	O(1)−Mg−O(2)	91.8(2)
N(1)−Mg−N(4)	70.77(14)	N(1)−Mg−N(3)	71.1(2)
O(2)−Mg−N(1)	107.4(2)	O(1)−Mg−N(1)	160.8(2)
N(1)−P(1)−N(3)	96.5(2)	N(2)−P(1)−N(3)	105.6(2)
N(2)−P(2)−N(4)	106.1(2)	N(1)−P(2)−N(4)	95.8(2)
P(1)−N(1)−P(2)	98.4(2)	P(1)−N(2)−P(2)	100.3(2)
N(1)−P(1)−N(2)	80.7(2)	N(1)−P(2)−N(2)	80.4(2)

endo orientation, that is, they are positioned directly above the $(P-N)_2$ ring. This is in contrast to their disposition in the related disulfide [(^{t}BuNPS)$_2$(^{t}BuNH)$_2$], where they adopt an exo-endo orientation.[7b] The *tert*-butyl substituents of the imide nitrogen atoms are bent slightly below the plane of a ring that exhibits a noticeable folding along the C(1)N(1)N(1A)C(1A) axis. This deformation has splayed the *tert*-butylamino P−N bonds and caused a comparatively wide separation of the donor atoms, 4.12 Å. Such ring distortions are common among *cis*-cyclodiphosph(III)azanes, and they may be caused by repulsive lone pair−bond pair interactions.[14] The P−N−P and N−P−N bond angles of 97.83° and 80.88° and the significant pyramidalization (347.73°) of the nitrogen atoms attest to substantial angle strain within the ring.

(14) (a) Wagner, A. J.; Vos, A. *Acta Crystallogr.* **1968**, *B24*, 1423. (b) Cameron, T. S.; Howlett, K. D.; Prout, C. K. *Acta Crystallogr.* **1977**, *B33*, 119.

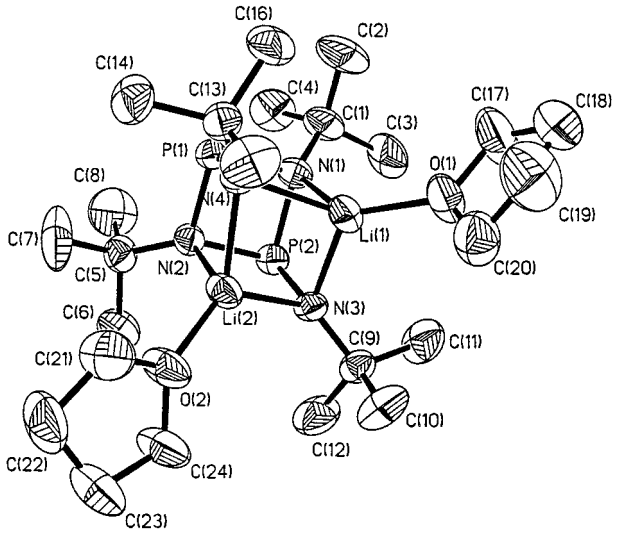

Figure 2. Perspective view of the heterocubic dilithio derivative **2a**. The 50% probability ellipsoids are shown.

The non-symmetry-related, but chemically equivalent, intraannular P−N bonds of **1a** are longer, 1.721(2) and 1.730(2) Å, than the exocyclic P−N bonds, 1.664(2) Å. Phosphorus−nitrogen single bonds in acyclic aminophosphines fall in the range 1.68−1.77 Å, the P−N bonds in tris(dimethylamino)-phosphine being a typical example, 1.700(5) Å.[15] In sterically congested cyclodiphosphazanes, for example, *trans*-{[(Me$_3$-Si)$_2$N]$_2$(PNSiMe$_3$)$_2$}, P−N(endo) = 1.727 and P−N(exo) = 1.712 Å were found,[16] while the P−N bonds in the less sterically encumbered *cis*-(^{t}BuNPCl)$_2$[17] are somewhat shorter, 1.689(4) Å. The P−N bonds in **1a** thus appear to be typical single bonds.

While we were in the final stages of submitting this manuscript we learned that a single-crystal X-ray study of serendipitously prepared *cis*-**1a** had recently been published.[18] The gross structural features derived from that study are the same as those reported in this paper, but there are disturbing inequivalences in the derived lengths of chemically equivalent bonds. Thus, for example, the exocyclic P−N bonds were found to be 1.619(6) and 1.710(5) Å, respectively. We believe these large variations to be due to the incorrect assignment and the subsequent refinement of the structure in the acentric space group *Pc*.

A single-crystal analysis on **2a**, Figure 2, showed it to be an inorganic heterocube of approximate C_{2v} symmetry. This molecular complex is composed of alternating nitrogen, phosphorus, and lithium atoms that are surrounded by a shell of organic groups. Crystal parameters and selected bond distances and angles are given in Tables 1 and 2, respectively. Within the cube all but the phosphorus atoms are four-coordinate, and all atoms achieve an electron octet through formation of covalent bonds, donor bonds, or lone pairs. Although the exocyclic P−N bonds are similar to those in the pristine molecule, the endocyclic bonds are slightly longer due to the steric congestion. Four crystallographically distinct, but equidistant, Li−N bonds form the buckled $(Li-N)_2$ ring whose bonds range from 2.077-(5) to 2.094(5) Å. These are of lengths similar to those in related lithium amides, compare {Li[N(SiMe$_3$)$_2$]OEt$_2$}$_2$ and Li−N =

(15) Vilkov, L. V.; Khaikin, L. S.; Erdokimov, V. V. *J. Struct. Chem. (Engl. Transl.)* **1969**, *10*, 978.
(16) Niecke, E.; Flick, W.; Pohl, S. *Angew. Chem., Int. Ed. Engl.* **1976**, *15*, 309.
(17) Muir, K. W. *J. Chem. Soc., Dalton Trans.* **1975**, 259.
(18) Reddy, N. D.; Elias, A. J.; Vij, A. *J. Chem. Soc., Dalton Trans.* **1997**, 2167.

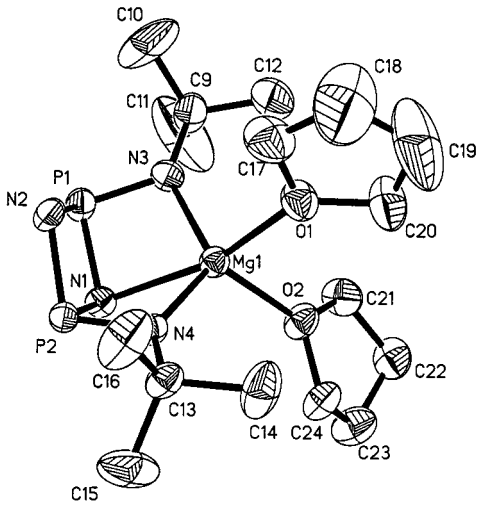

Figure 3. Perspective view of the seco-heterocubic magnesium complex **3a**, showing the 50% thermal ellipsoids of the non-hydrogen atoms. To enhance clarity, the *tert*-butyl groups on the imido nitrogen atoms have been omitted.

2.06(1) Å,[19] but they are shorter than the Li−N donor bonds, 2.104(5) and 2.121(5) Å. The considerable ring distortion, angle sum = 351.2°, is in contrast to the perfectly planar $(P-N)_2$ ring, angle sum = 359.6°, and is due to the presence of the disproportionally large lithium atoms.

Figure 3 shows a perspective ORTEP drawing of the almost C_s-symmetric **3a** that emphasizes the coordination geometry about the magnesium atom. The crystal data are summarized in Table 1, and selected bond lengths and angles are listed in Table 2. This complex is related to **2a** by the formal replacement of two lithium atoms by one magnesium atom and approximates a seco-heterocube, that is, a heterocube with a missing corner. As the result of its location in the cube, the magnesium atom has a highly distorted trigonal bipyramidal environment, being coordinated by three cyclodiphosphazane nitrogen atoms and two THF oxygen atoms. While the metal−nitrogen bonds to the perfectly trigonal-planar N(3) and N(4) are identical and of normal lengths,[3b] 2.059(4) and 2.061(4) Å, the N(1)−Mg donor bond is considerably longer, 2.330(4) Å. The slightly inequivalent Mg−O bonds, 2.070(4) and 2.095(4) Å, enclose an angle of 91.8(2)°. There is a small, but statistically significant, increase in the P−N bond lengths to the 4-coordinate nitrogen atom N(1). The orientation of the tetrahydrofuran molecules with respect to the oxygen−metal plane reveals substrate selectivity, as the THF molecule near the open corner of the cube is parallel to the Mg−O(1)−O(2) plane, while the second THF molecule is perpendicular to it.

Discussion

We are investigating chelating bis(amido) ligands that provide well-defined coordination environments for olefin-polymerization catalysts and have identified alkylamino-substituted inorganic ring compounds, particularly $(Si-N)_2$ and $(P-N)_2$ systems, as good candidates. These heterocycles are quintessential ancillary ligands, because they are stable and easy to synthesize and have a selective coordination gap.

Although the useful ligating properties of bis(alkylamido)-cyclodisilazanes in main-group metal chemistry are well-established,[3] the involved syntheses justify their use only in those cases where the potential benefits are reasonably well-established. In order to speed up the catalytic screening of cyclodisilazane complexes, we have been searching for structural analogues that can be synthesized more easily.

Bis(alkylamino)cyclodiphosphazanes and -cyclodisilazanes have isoelectronic (P = Si−Me) central cages and thus presumably similar ligating properties. The phosphorus−nitrogen heterocycles, however, are much easier to prepare than their silicon counterparts, often being accessible in one- or two-step syntheses. This should expedite studies of their coordination chemistry and facilitate the identification of complexes with interesting chemical properties. These findings would then be readily translatable to cyclodisilazane derivatives and lead to the development of a parallel (cyclodiphosphazane−cyclodisilazane) coordination chemistry. The viability of this approach depends, of course, upon a high degree of structural similarity between the two ligand systems.

The purpose of this work was therefore to synthesize and X-ray-structurally characterize cyclodiphosphazane complexes that are isoelectronic with proven cyclodisilazane ligands. We found, to our surprise, that, with the exception of one antimony[20a] and two tin complexes,[20b] no reports on metal derivatives of cyclodiphosphazanes had appeared previously.[21] It thus seemed reasonable to begin our studies with the easily accessible bis(*tert*-butylamino)cyclodiphosphazane, **1a**, and its lithium and magnesium salts. Table 3 lists some comparative bond lengths and angles for the cyclodiphosphazanes of this work and those of the corresponding cyclodisilazane derivatives.

Although the X-ray structural data on *cis*-bis(*tert*-butylamino)-cyclodisilazane, **1b**,[22] clearly show it to be isostructural with **1a**, the poorly refined data of this structure determination were unsuitable for metric comparisons and compelled us to use those

Table 3. Comparison of Selected Bond Lengths (Å) and Angles (deg) for **1a**−**3a** and **1b**−**3b**[a]

	1a	*trans*-**1b**
E−E	2.600(2)	2.5417(8)
E−N(imido), av	1.725(2)	1.7386(13)
E−N(amido), av	1.664(2)	1.7145(13)
N−E−N, av	80.00(11)	86.06(6)
E−N−E	97.83(11)	93.46(6)
	2a	**2b**
E−N(imido), av	1.778(2)	1.763(2)
E−N(amido), av	1.651(2)	1.672(2)
N−Li, donor bonds, av	2.113(5)	2.240(5)
N−Li, amide, av	2.086(5)	2.139(5)
Li−O, av	1.957(5)	1.988(5)
E···E	2.6620(10)	2.5452(10)
N−E−N, av ring	82.84(10)	85.78(10)
E−N−E, av ring	96.94(10)	92.44(10)
	3a	**3b**
E−N(imido), av	1.776(4)	1.744(7)
E−N(amido). av	1.656(4)	1.677(6)
N−Mg, donor bond	2.330(4)	2.704(6)
N−Mg, av	2.060(4)	2.094(6)
Mg−O, av	2.083(4)	2.115(6)
E···E	2.694(2)	2.537(4)
N−E−N, av ring	80.6(2)	84.9(3)
E−N−E, av ring	99.4(2)	93.3(3)

[a] E = P (**a**), SiMe (**b**).

(19) Lappert, M. F.; Slade, M. J.; Singh, A. *J. Am. Chem. Soc.* **1983**, *105*, 302.

(20) (a) Scherer, O. J.; Wolmershäuser, G.; Conrad, H. *Angew. Chem., Int. Ed. Engl.* **1983**, *22*, 404. (b) Linti, G.; Nöth, H.; Schneider, E.; Storch, W. *Chem. Ber.* **1993**, *126*, 619.

(21) Our communication on zirconium and hafnium complexes of **1a** was recently published, see: Grocholl, L.; Stahl, L.; Staples, R. J. *J. Chem. Soc., Chem. Commun.* **1997**, 1465.

(22) Grocholl, L.; Stahl, L. Work in progress.

of the much better refined ($R = 0.0459$) trans-isomer.[23] trans-**1b** has a planar four-membered $(Si-N)_2$ ring with intraannular and extraannular silicon−nitrogen bond lengths of 1.7385(12) and 1.7145(13) Å, respectively, and a transannular Si···Si separation of 2.5417(8) Å. While the E−N bonds (E = Si, P) follow size trends and are slightly longer in the silicon compound, the greater difference between the intra- and extraannular E−N bonds and the larger E···E separation in the cyclodiphosphazane may reflect lone-pair repulsions. With the exception of the E···E separations, the E−N bond lengths of *trans*-**1b** and **1a** are within about 0.05 Å of each other, although the significance of this difference is somewhat diminished by the use of data from the *trans*-cyclodisilazane in this comparison.

Table 3 shows selected bond lengths for the isostructural dilithio derivatives **2a** and **2b**. These heterocubes can be viewed as consisting of two four-membered $(E-N)_2$ and $(Li-N)_2$ rings joined by two E−N and two Li−N donor bonds. The intraannular and extrannular Si−N bond lengths of 1.764(2) and 1.670(2) Å compare very well with the corresponding values in **2a**, 1.778(2) and 1.651(2) Å. Given the smaller size of the phosphorus atom, one would again expect slightly shorter bonds in the cyclodiphosphazane complex, and this is generally borne out by the data, although the longer intraannular P−N bonds are a noteworthy exception. These trends extend to the four lithium−nitrogen bonds in the $(Li-N)_2$ portion of **2b**, which range from 2.120(5) to 2.160(5) Å.[23] Their average value of 2.139(5) Å is longer than that in **2a**, 2.086(5) Å, and a similar observation can be made for the two Li−N donor bonds. Because the lithium derivatives are truly isostructural—their bond lengths are generally within 8σ of each other—the isostructural nature of these compounds is even more apparent than that of **1a** and **1b**.

The magnesium complexes **3a** and **3b** show the greatest variation in overall geometry among the three isoelectronic pairs of this study. Whereas the metal atom is pseudotetrahedrally coordinated in the cyclodisilazane analogue,[3b] its inclusion in the heterocube makes it 5-coordinate in **3a**. It is not clear, however, whether this change in coordination environment is the cause or the effect of the much greater transannular E···E distance in **3a**, 2.694(2) versus 2.537 Å. In keeping with the trends observed in dilithio derivatives, the intraannular E−N distances are shorter in the cyclodisilazane complex while the extraannular E−N bonds are shorter in the cyclodiphosphazane derivative. Despite the comparatively large overall differences of both molecules, their bond lengths rarely differ by more than 0.03 Å. Presumably due to inductive effects, the magnesium−amide bonds, 2.059(4) Å versus 2.094(6) Å, and magnesium−THF bonds, 2.083(4) versus 2.115(6) Å, are shorter in the phosphazane complex.

Although limited in scope, these data do show emerging trends that provide the basis for some generalizations. Metal-nitrogen, metal−oxygen, and exocyclic E−N bonds tend to be shorter in the cyclodiphosphazane complexes, while the intraannular E−N and E−E bonds are shorter in the cyclodisilazane derivatives. The shorter exocyclic E−N and M−N bonds can be rationalized in terms of the phosphorus atom's smaller size and inductive effects, but lone pair−lone pair repulsions may be responsible for the longer endocyclic P−N bonds in **2a** and **3a**. One of the most surprising trends is the steady increase in the nonbonded P···P distances of the cyclodiphosphazane species, which range from 2.600(2) Å in the free ligand to 2.694(2) Å in the magnesium complex. This lengthening is in notable contrast to the almost constant transannular Si···Si distances in the cyclodisilazane derivatives, and it may reflect the comparative weakness of these P−N bonds.

The multitude of bond angles makes a detailed discussion of their numerical values impractical, but the common $(E-N)_2$ moiety provides a good basis for a limited number of such comparisons, some of which are listed in Table 3. The endocyclic N−P−N angles in **1a**−**3a** are fairly constant, ranging from 80.6(2) to 82.84(10), and they are consistently 4−5° smaller than the corresponding N−Si−N angles. This lone pair induced compression may have caused the distortions of the rhombic ring, resulting in wider P−N−P angles and larger E···E separations.

Structural aspects are, of course, only one of the factors to consider when comparing analogous compounds. We have largely avoided a discussion of the electronic influences in these heterocyclic ligands, because they are much more difficult to quantify. Phosphorus is more electronegative than silicon, and its compounds should have shorter M−N and M−O bonds and more Lewis acidic metal centers. This is indeed observed in the complexes of the cyclodiphosphazane. In the pristine molecules, **1a** and **1b**, inductive influences are clouded by lone pair effects, however, as demonstrated by the lack of clear trends in the $(P-N)_2$ bond lengths. These poorly defined electronic factors may ultimately pose the greatest obstacle for the development of a parallel coordination chemistry of both ligands, perhaps the most important being the phosphorus lone-pair electrons that may interfere with strongly Lewis-acidic reagents.

Conclusion

A bis(*tert*-butylamino)-substituted cyclodiphosphazane has allowed the synthesis of lithium and magnesium complexes that are isostructural with those of the isoelectronic cyclodisilazane, confirming that both ligands can form isostructural coordination compounds. The much greater ease of synthesizing and modifying cyclodiphosphazanes should make them even more attractive ligands than cyclodisilazanes, and we are currently investigating their chemistry with a wide variety of elements.

Acknowledgment. This work was supported by grants from the University of North Dakota and North Dakota EPSCoR.

Supporting Information Available: Three X-ray crystallographic files, in CIF format, are available on the Internet. Access information is given on any current masthead page.

(23) Staples, R. J.; Grocholl, L.; Stahl, L. Manuscript in preparation.

IC971201F